

## REDUCTION OF NO<sub>x</sub> IN A DIESEL ENGINE USING SPLIT INJECTION APPROACH

P. KRISHNA<sup>1</sup>, A. K. BABU<sup>2</sup>, A. P. SINGH<sup>3,\*</sup>, A. A. RAJ<sup>1</sup>

<sup>1</sup>Department of Mechanical Engineering, Easwari  
Engineering College Chennai, Tamilnadu, India

<sup>2</sup>Department of Mechanical Engineering, PERI Institute of  
Technology Chennai, Tamilnadu, India

<sup>3</sup>Production Engineering Department, College of Engineering,  
Defence University Bishoftu, Ethiopia, Africa

\*Corresponding Author: singh\_ajit\_pal@hotmail.com

### Abstract

One of the important goals in diesel engine research is the development of means to reduce the emissions of oxides of nitrogen (NO<sub>x</sub>) and soot particulates, and in this endeavour advanced techniques like split injection/multiple injection, exhaust gas recirculation (EGR) etc. are being developed. The principle of split injection is that when fuel is injected in two pulses it engenders a reduction in the peak combustion chamber temperature which ensures the reduction in NO<sub>x</sub> emission. In this study to achieve split injection in an economical manner, a double lobed cam has been designed incorporating the optimum split and dwell. Experimental study indicates that 50-50 split with 10 degree crank angle dwell is the optimum to achieve a viable reduction in NO<sub>x</sub> without any major penalty in soot and power. A 15% reduction in NO<sub>x</sub> and 10% reduction in soot was observed on incorporating these results.

Keywords: Diesel engine, NO<sub>x</sub>, Soot, Split injection.

### 1. Introduction

Diesel engines have been very popular for heavy duty application for both on-road and off road for its robustness and its ability to produce high torque. However, with stricter emission regulations diesel engine manufactures have found it very difficult to attain a balance between cleaner emissions, better fuel economy and higher thermal efficiencies. One of the biggest challenges that engine

**Nomenclatures**

$b$	Face width of cam, m
$d^2y/dt^2$	Acceleration of cam
$E_1, E_2$	Young's modulus of cam and follower, N/m <sup>2</sup>
$F_n$	Normal load, N
$h$	Maximum rise of follower, m
$R_b$	Radius of base circle, m
$R_p$	Radius of prime circle of cam, m
$R_r$	Radius of roller, m
$y$	Rise of follower, m

**Greek Symbols**

$\beta$	Cam angle for rise $h$ , radian
$\rho_c$	Minimum radius of cam, m
$\omega$	Angular speed of cam, rpm
$\theta$	Cam angle for displacement $y$ , radian

**Abbreviations**

BSFC	Brake Specific Fuel Consumption
BTE	Brake Thermal Efficiency
CO	Carbon Monoxide
CO <sub>2</sub>	Carbon Dioxide
EGR	Exhaust Gas Recirculation
HSDI	High-Speed Direct Injection
ITE	Indicated Thermal Efficiency
ME	Mechanical Efficiency
NO	Nitrogen Oxide
NO <sub>x</sub>	Oxides of Nitrogen
PM	Particulate Matter
SFC	Specific Fuel Consumption
TDC	Top Dead Center
TFC	Total Fuel Consumption
UBHC	Un-Burnt Hydrocarbons

manufacturers have been facing is the trade-off between NO<sub>x</sub> and particulate matter (PM) formation. As a result advanced combustion has been identified as one of the ways by which NO<sub>x</sub>-PM can be simultaneously reduced without increasing fuel penalty. Advanced combustion in a diesel engine can be achieved by varying engine parameters such as fuel injection timing, and number of fuel injection.

Exhaust emissions are just the by-products of combustion of a fuel (diesel). For every 1 kg of fuel burnt, there is about 1.1 kg of water (as vapour/steam) and 3.2 kg of carbon dioxide (CO<sub>2</sub>) produced. Complete combustion is not practically

observed. Hence unwanted gases such as carbon monoxide (CO) and un-burnt hydrocarbons (UBHC) are emitted. In addition, the high temperatures that occur in the combustion chamber of a diesel engine promote an unwanted reaction between nitrogen and oxygen from the air. This result in formation of various oxides of nitrogen, commonly called NO<sub>x</sub>.

Extensive research is in progress to reduce NO<sub>x</sub> and soot emissions from a diesel engine due to environmental concerns. One of the emission control strategies is in-cylinder reduction of pollutant production. It is well known that it is very difficult to reduce both NO<sub>x</sub> and soot production simultaneously during the combustion process. Many emission reduction technologies developed so far tend to increase soot emission while reducing NO<sub>x</sub> emission and vice-versa. For example retarding fuel injection timing can be effective to reduce nitrogen oxide (NO) formation. However, this usually results in an increase of soot production on the other hand although increasing fuel injection pressure can decrease soot emission it can also cause higher NO<sub>x</sub> emission at same time [1]. Recently, it has been experimentally shown that with high pressure multiple injections, the soot-NO<sub>x</sub> trade off curves of a diesel engine can be shifted closer to the engine than with single pulse injection, reducing both soot and NO<sub>x</sub> emission significantly [2-4].

In split injection, the fuel is injected in two pulses which leads to reduction in ignition delay. This results in the greater fraction of combustion to occur in the expansion stroke. Since the majority of the NO<sub>x</sub> is formed in the premixed combustion, the net amount of NO<sub>x</sub> produced in split injection is reduced. It has been found that by varying the amount and the time period between the two pulses it is possible to reduce simultaneously soot and NO<sub>x</sub> emissions.

Nehmer and Reitz [2] experimentally investigated the effect of double pulse/split injection on soot and NO<sub>x</sub> emission using a single cylinder Caterpillar heavy duty diesel engine. They varied the amount of fuel injected in the first injection pulse from 10%-75% of the total amount of fuel and found that split injection affected the soot- NO<sub>x</sub> trade off. In general their split injection scheme reduced NO<sub>x</sub> with only a minimal increase in soot emission and did not extend combustion duration.

Tow et al. [3] continued the study of Nehmer and Rietz [2] using the same engine and included different dwells between the injection pulses. They found that at high engine load (75%) particulate will be reduced by a factor of 3 with no increase in NO<sub>x</sub> and only 2.5% increase brake specific fuel consumption (BSFC) compared to a single injection using a double injection with a relatively long dwell between injection. Another important conclusion was that dwell between injection pulses was very important to control soot production and there exists an optimum dwell at a particular engine operating condition. The optimum dwell of a double injection was found to be about 10° crank angle at 75% load and 1600rpm for their engine condition.

Pierpont et al. [1] confirmed that amount of fuel injected in the first pulse affect the particulate level where the NO<sub>x</sub> emission level was held constant. The best double injections were found to be those with 50%-60% of the fuel injection in the first pulse. They also found that with a combination of EGR and multiple

injections, particulate and NO<sub>x</sub> were simultaneously reduced to as low as 0.07 and 2.2 g/bhp-hr respectively at 75% load and 1600 rpm.

Han et al. [5] observed that when the 50-8-50 double injection with a dwell period used, both the soot and NO emission are reduced below those of the single case however when the 25-8-75 double injection is used the soot emission increase significantly at the same time NO emission is reduced greatly. They concluded that the NO reduction mechanism is found similar to that of single injection with retarded injection timing. Soot formation is reduced after the injection pause between the injection pulses. The reduced soot formation is shown to be the fact that the soot producing rich regions at the spray tip are no longer replenished. During the dwell between injection pulses the mixture becomes leaner.

Gao and Schreiber [6] concluded that only the 50-8-50 split fuel ratio adds any advantage to the base line case for improving the soot- NO<sub>x</sub> trade off. Miles and Dec [7] concluded that split injection can lead to large increase flame surface which in turn may increase mixing and soot oxidation thereby lowering emissions. Pilot injection strategies are unlikely to achieve significant noise reduction at low temperatures which prevail in cold start condition. They also observed that pilot injection is effective in reducing the noise levels in high-speed direct injection (HSDI) engines but can lead to unstable combustion behaviour.

According to CFD modelling multiple injections were found to be most effective in reducing particulate and NO<sub>x</sub> [8]. Babu and Devaradjane [9] by mathematical modelling concluded that 30-70 coupled with crank angle spacing of 5° offers the optimum solution particularly for reducing the emissions of NO with a marginal loss of power and thermal efficiency.

In accordance with the above reviews, it is observed that a 50-50 split with 10° crank angle dwell will be the optimum to achieve NO<sub>x</sub>-soot trade off without a penalty in power and thermal efficiency for the engine. Thus a double lobbed cam is designed to achieve the above stated conditions in a split injection fuel system model.

## **2. Materials and Method**

### **2.1. Design of double lobbed cam**

The important aspect of a cam design is the kinematics of the cam. The following calculations were carried out to determine the actual cam profile and to design the modified cam.

#### **2.1.1. Actual cam profile**

The actual cam profile was obtained by using a cam measuring apparatus. The corresponding profile was developed from the displacement-angle graph as shown in Table 1 and Fig. 1. It was inferred from the graph that the cam is of constant velocity over the injection and suction period of the pump were calculated using the engine specification and the displacement angle diagram.

It noted that the displacement varied linearly after the start of injection around  $-25^\circ$  from the top dead center (TDC) and then reached the height of 8.1mm at  $15^\circ$  from the TDC where the injection stopped and the suction continued for the next  $120^\circ$  of the cam angle, this is inferred from the displacement angle diagram.

**Table 1. Displacement Variations with Cam Angle.**

Cam angle (degrees)	Displacement (mm)	Cam angle (degrees)	Displacement (mm)
0	0.05	180	8.1
20	0.05	200	5
100	0.05	214	2.5
120	0.05	220	1.5
140	0.05	232	0.05
160	1.25	240	0.05
168	2.75	280	0.05
170	4	300	0.05
172	5.5	360	0.05

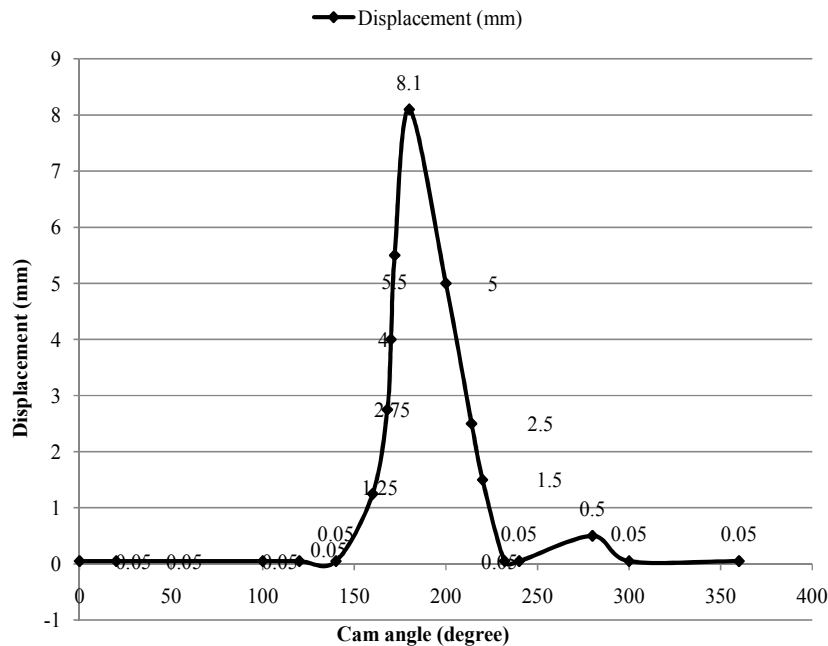


**Fig. 1. Variation of Displacement with Cam Angle.**

Figure 2 represents the three dimensional (3-D) view of the cam. It was obtained by plotting the displacement for the corresponding angle in the polar co-ordinate system, using the CATIA V5 software as shown in Fig. 3. Figure 4 represents the various two dimensional (2-D) view of the cam profile.

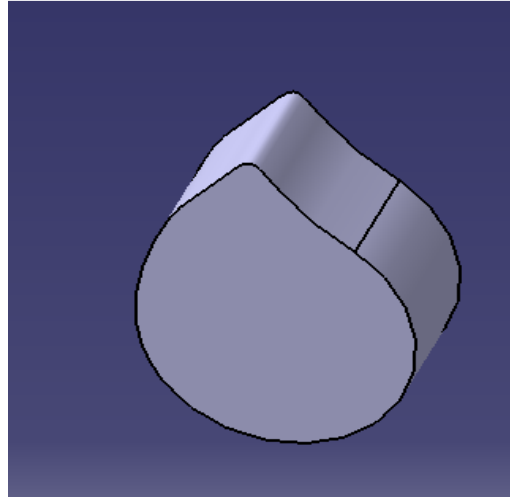


**Fig. 2. Three Dimensional View of Actual Cam.**

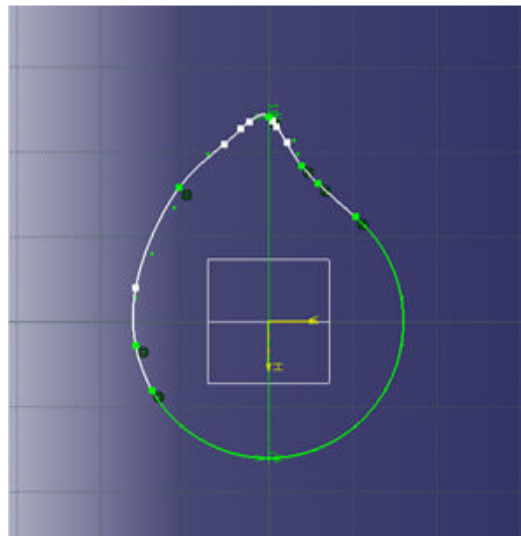


**Fig. 3. Polar Co-ordinate Diagram.**

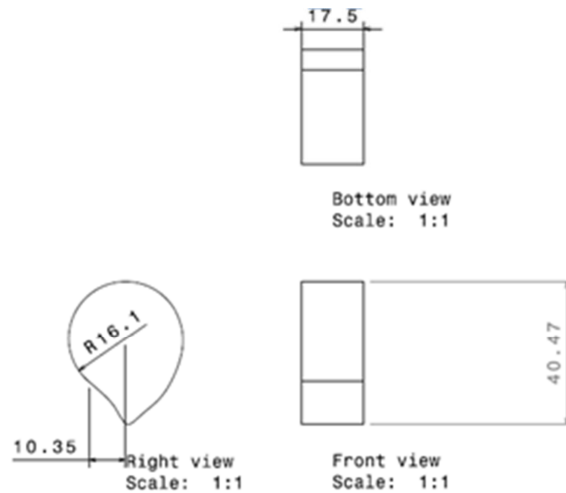


**Fig. 4. Actual Cam Views.**

### 2.1.2. Modified cam profile

The design of a modified cam was based on the literature review that the injection with 50-50 split and  $10^\circ$  crank angle dwell is the best suited for trade-off between emission control and fuel penalty. A constant velocity motion was chosen for each of lift. The characteristics of the modified cam as shown in Fig. 5 have been specified as follows.

- Proposed dwell  $5^\circ$  cam angle,
- Constant velocity for each lift similar to original cam,
- Each lift is for  $7.5^\circ$  cam angle,
- Time period for dwell is 1.11 millisecond,
- Time period for split injection is 3.3 millisecond (1.665 millisecond per pulse),
- The suction period remains the same as the actual cam.

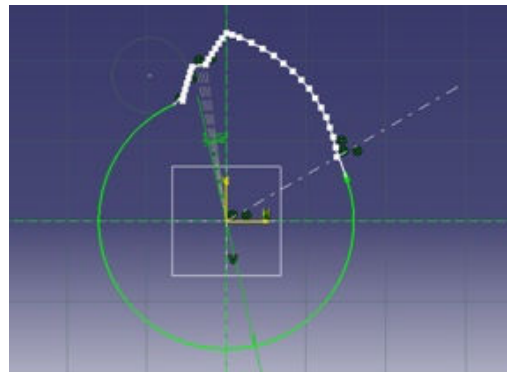


**Fig. 5. Polar Co-ordinate Diagram of Modified Cam.**

Figures 6 and 7 represents the 3-D view of the modified cam which is plotted from the displacement versus angle graph as shown in Table 2 and Fig. 8 using the constant velocity interpretation.

The design of the return stroke remains the same as it does not impact the injection. As per the design the first impulse occur from  $160^{\circ}$ - $167.5^{\circ}$  then a dwell between  $167.5^{\circ}$ - $172.5^{\circ}$  and the remaining fuel is injected from  $172.5^{\circ}$ - $180^{\circ}$ . As the displacement is split in equal halves, the 50-50 ratio is achieved.

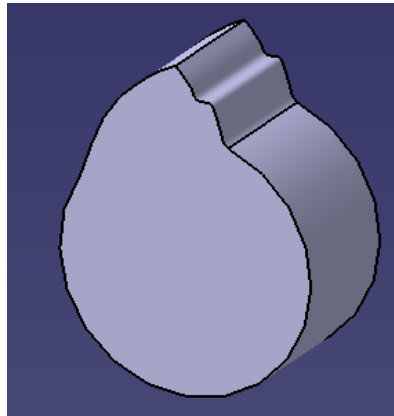


Fig. 6. Three Dimensional View of Modified Cam.

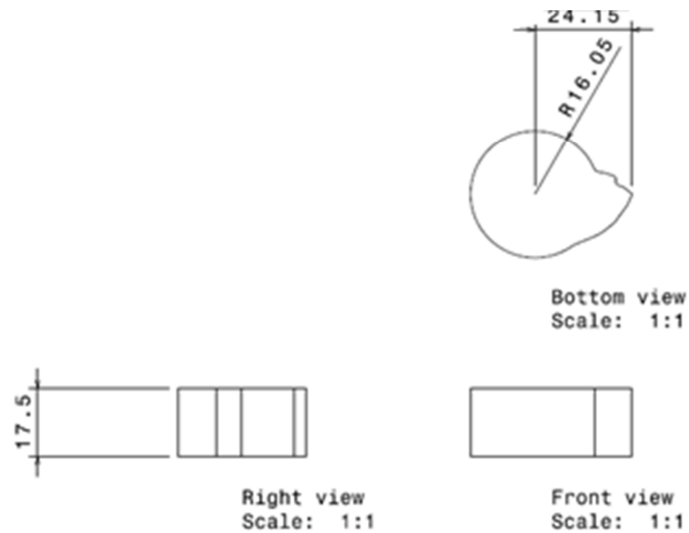
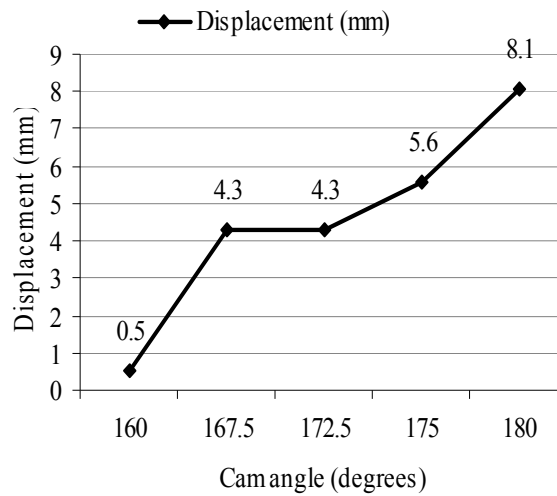


Fig. 7. Modified Cam Views.



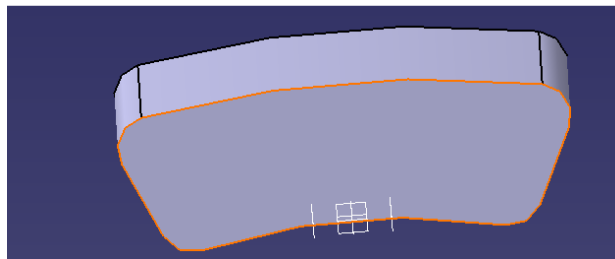
**Table 2. Cam Angle Versus Displacement**

Cam angle (degrees)	Displacement (mm)
160	0.5
167.5	4.3
172.5	4.3
175	5.6
180	8.1

**Fig. 8. Variation of Displacement with Cam Angle (Extension Stroke only).**

### 2.1.3. Rocker arm (follower) design

The rocker arm face was modified in order to avoid two points of contact and also to avoid the cam from locking. It is to avoid any violation of the cam profile movement by the follower. The design of the rocker face was based on a trial and error method to find out the optimum size and profile of the follower face. This was done using CATIA V5 software starting with the actual follower as the base as shown in Figs. 9-12.

**Fig. 9. Three Dimensional Diagram of a Rocker Arm.**

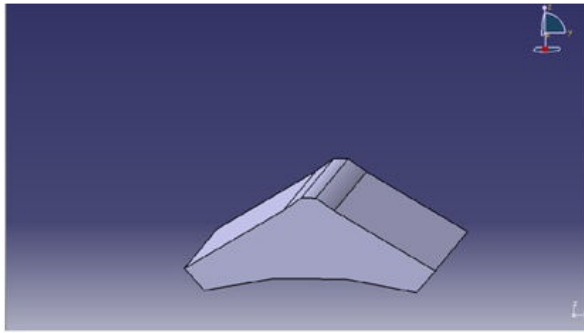


**Fig. 10. Three Dimensional Diagram of a Modified Rocker Arm.**



**Fig. 11. Photograph of a Modified Cam (Double Lobbed Cam).**



**Fig. 12. Photograph of a Modified Follower.**

### 2.1.4. Force analysis

The force analysis was conducted on the cam to determine whether the new design and the material chosen would be able to withstand the stresses of the operation. Stress acting on the cam is contact stress and this can be calculated as follows.

Contact stress [10-12] can be calculated by using Eq. (1).

$$\sigma_c = 0.591 \sqrt{\frac{F_n E_1 E_2 \left( \frac{1}{R_r} \pm \frac{1}{\rho_c} \right)}{b(E_1 + E_2)}} \quad (1)$$

where,  $F_n$  - normal load, N;  $b$  - face width of cam in meters (measured) =  $17.5 \times 10^{-3}$  m;  $E_1, E_2$  - Young's modulus of cam and follower in  $\text{N/m}^2$ ;  $\rho_c$  - minimum radius of cam in meters;  $R_r$  - radius of roller in meters (for flat face follower radius is considered as infinite); and  $P$  - Pressure of the pump  $\times$  Area of piston.

Material proposed to be used is 40Cr1Mo28, Hardness=270-300 BHN (Heat treated). Since a flat follower has been used,  $R=\infty$  for the model proposed here.

Calculation of the minimum radius of the cam [10-12] as per Eq. (2).

$$\rho_c = R_b + \left( y + \frac{1}{\omega} \times \frac{d^2 y}{dt^2} \right) \quad (2)$$

where,  $R_b$ -radius of base circle in meters;  $y$ -rise of follower in meters;  $\omega$ -angular speed of cam in rpm;  $d^2 y/dt^2$ -acceleration of cam;  $y=h\theta/\beta$ ;  $\theta$ -cam angle for displacement  $y$  in radian;  $\beta$ -cam angle for rise  $h$  in radian;  $h$ -maximum rise of follower in meters.

Calculation of  $dy/dt$ :

$$\frac{\beta}{4h\omega} \frac{dy}{dt} = 0.5 \quad (3)$$

$$\frac{dy}{dt} = \left( \frac{dy}{dt} \right)_{\max} \quad (4)$$

As the motion is of constant velocity as shown in Fig. 8, to find maximum pressure angle [10-12]:

$$\tan \alpha_{\max} = \left( \frac{dy}{dt} \right)_{\max} \div (R_p + y)\omega \quad (5)$$

where,  $R_p$ -radius of prime circle of cam= $R_b+R_r$ ;  $R_b$ -radius of base circle of cam;  $R_r$ -radius of roller (point contact mushroom follower).

$$\rho_{k \min} = \frac{\left[ (R_p + y)^2 + \left( \frac{1}{\omega} \times \frac{dy}{dt} \right)^2 \right]^{3/2}}{\left[ (R_p + y)^2 + 2 \left( \frac{1}{\omega} \times \frac{dy}{dt} \right)^2 - (R_p + y) \right] \times \left( \frac{1}{\omega^2} \times \frac{d^2y}{dt^2} \right)}$$

$$\rho_c = R_b + y \quad (6)$$

### 3. Experimental Setup

A single cylinder, four-stroke, water cooled, direct injection, constant speed, compression ignition engine developing power output of 3.7 kW was used for this work as shown in Fig. 13.

Test engine specifications are given in Table 3. A pony brake was used for loading the engine. The performance test and emission test were carried out on both the modified and the standard engine. The result of the standard engine has been used as the base.

The emission test was carried out at rated condition using an AVL make 5 gas analyzer ensuring that the testing condition-the humidity and the water flow rate remain the same for both the standard and modified engine.

The performance test was carried out by varying the load applied to the engine using pony brake. The brake thermal efficiency, the indicated thermal efficiency and the mechanical efficiency were computed.



**Fig. 13. Engine Setup for the Experimentation.**

**Table 3. Test Engine Specifications.**

Type of engine	Single cylinder, direct injection diesel engine
Power	5 hp/3.7 kW
Speed	1500 rpm
Make	Anil
Injector	3-point injector
Fuel pressure	160 bar

#### 4. Fabrication

The main aspect of fabrication in the project is the machining of the cam and the rocker arm to the required profile. The outline of the steps followed has been described in the flowchart as shown in Fig. 14.

The timing gear was marked while removing the cam shaft for reference during assembly. Then the actual cam profile was measured using the cam measuring apparatus. The cam profile was ascertained by plotting the displacement-cam angle graph. Based on the profile of this cam the double lobed cam was designed. The rocker arm profile was generated using CATIA V5 and the design profile on the cam was obtained using grinding.

In order to obtain the modified cam profile ZEDALLOY 350 (Manufacturers D & H) was added using arc welding and the required profile was generated by grinding. The modified cam shaft was assembled back into the engine using the previously marked point as reference in order to avoid any change in timing.

#### 5. Results and Discussion

The performance and emission tests were carried out before and after modification to analyze the effect of split injection. The results have been compared and discussed as follows.

##### 5.1. Emission test

The emission test was performed on the engine using a 5-gas analyser. The results have been tabulated in Table 4. It was observed that 14.2% reduction of  $\text{NO}_x$  was observed which is in-line with the expectation from a split injection of 50-10-50 along with a 11.43% reduction of UBHC at no load condition. A partial increase in the CO is observed due to partial combustion of the fuel in the later stages of combustion. This can be easily reduced by exhaust gas treatment.

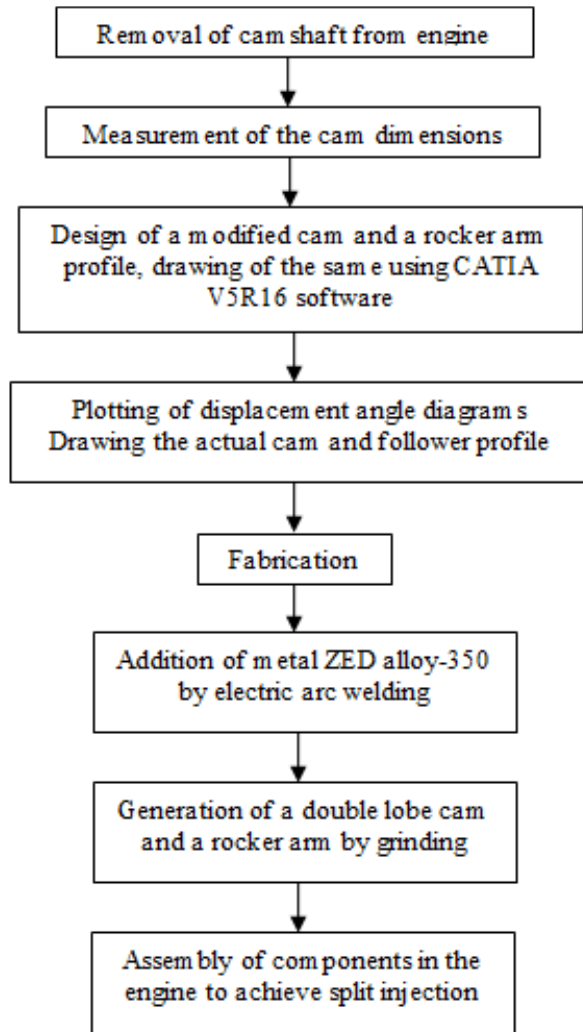


Fig. 14. Flow Chart for Fabrication.

Table 4. Emission Test Results.

Exhaust gas	Before modification	After modification	Percentage change
CO	0.08%vol.	0.09%vol	16.66
HC	76ppm	67ppm	-11.8
NO	135ppm	116ppm	-14.1
CO <sub>2</sub>	2.5%vol.	2.6%vol	4
O <sub>2</sub>	13.5%vol.	14%	3.7

## 5.2. Performance test

The performance test was carried out using a pony brake apparatus as shown in Fig. 15. The comparison between the various engine parameters such as (a) specific fuel consumption (SFC), (b) brake thermal efficiency (BTE), (c) indicated thermal efficiency (ITE) and (d) mechanical efficiency (ME) between the standard and the modified engine were carried out to determine the effectiveness of split injection as emission control method.

### 5.2.1. Specific fuel consumption versus brake power

Figure 15 show the variation of the SFC with the varying load condition. It is observed that the SFC for the modified engine with split injection does not vary considerably when compared with the standard. Hence it is ascertained that the fuel economy of the engine is not affected much due to split injection.

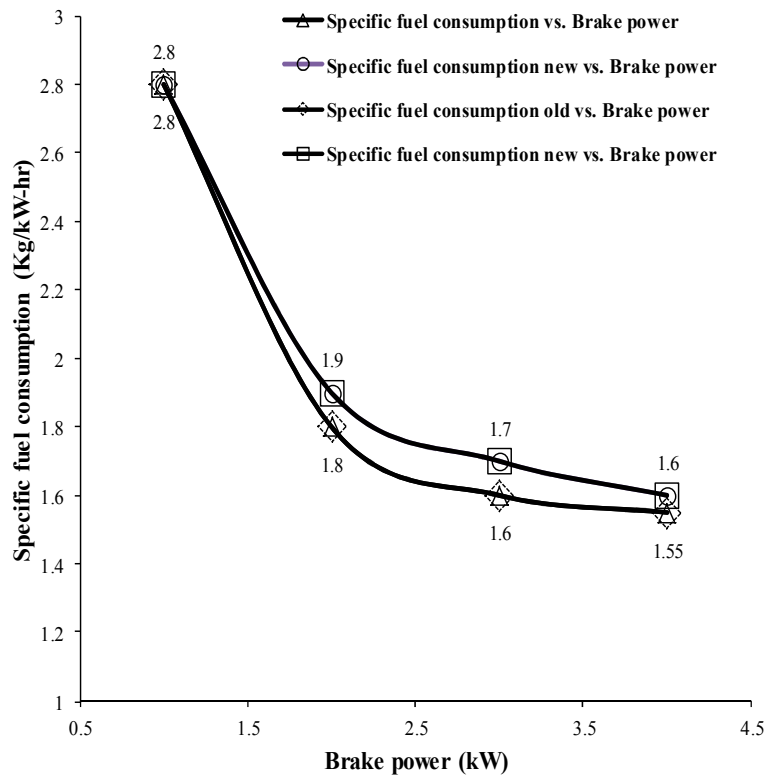


Fig. 15. Variation of Specific Fuel Consumption vs. Brake Power.

### 5.2.2. Brake thermal efficiency versus brake power

It is observed the brake thermal efficiency of an engine with 50-10-50 split injection of fuel remains almost same as that of the single injection engine

and slightly decreases at higher loads as shown in Fig. 16. This signifies that the modified engine with the split injection, i.e., the new engine is as efficient as the old one.

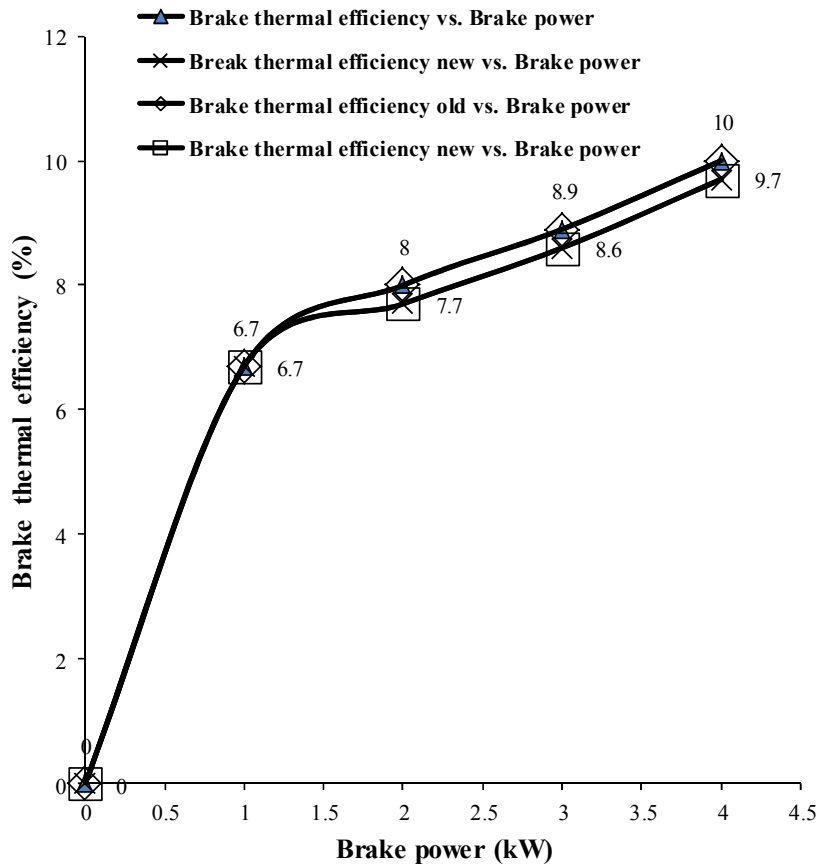


Fig. 16. Variation of Brake Thermal Efficiency vs. Brake Power.

**5.2.3. Indicated thermal efficiency versus brake power**

The frictional power was obtained by extrapolating Fig. 17. The negative value of brake power at which the total fuel consumption (TFC) is zero is equal to the frictional power. In both the modified and unmodified engine the frictional power was found out to be approximately equal to 0.9 kW.

Indicated thermal efficiency signifies the theoretical efficiency that would be obtained as per the indicator diagram. It is conceived from Fig. 18 that the indicated thermal efficiency of modified engine when compared with that of the standard is lower. This is expected as the peak combustion temperature is reduced in case of split injection.



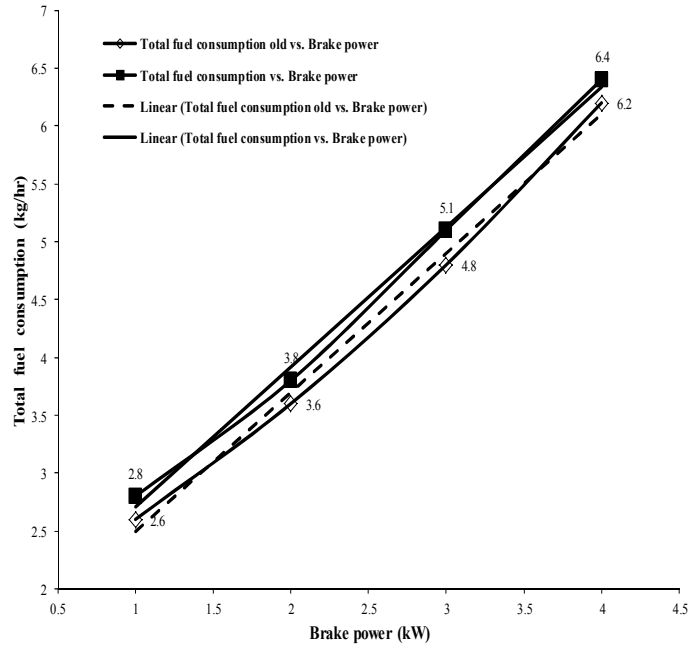


Fig. 17. Variation of Total Fuel Consumption vs. Brake Power.

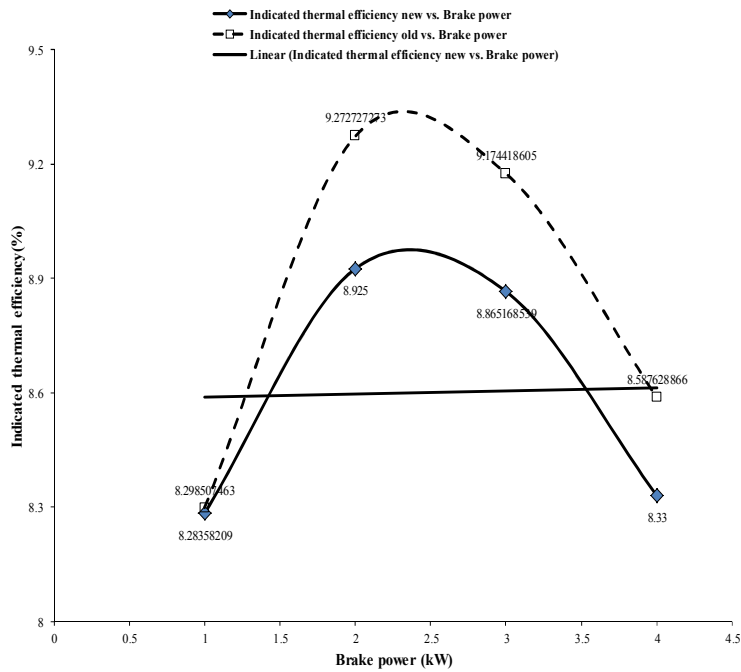


Fig. 18. Variation of Indicated Thermal Efficiency vs. Brake Power.

### 5.2.4. Mechanical efficiency versus brake power

Figure 19 shows that the mechanical efficiency of the engine with 50-8-50 split injection and the normal engine are the same.

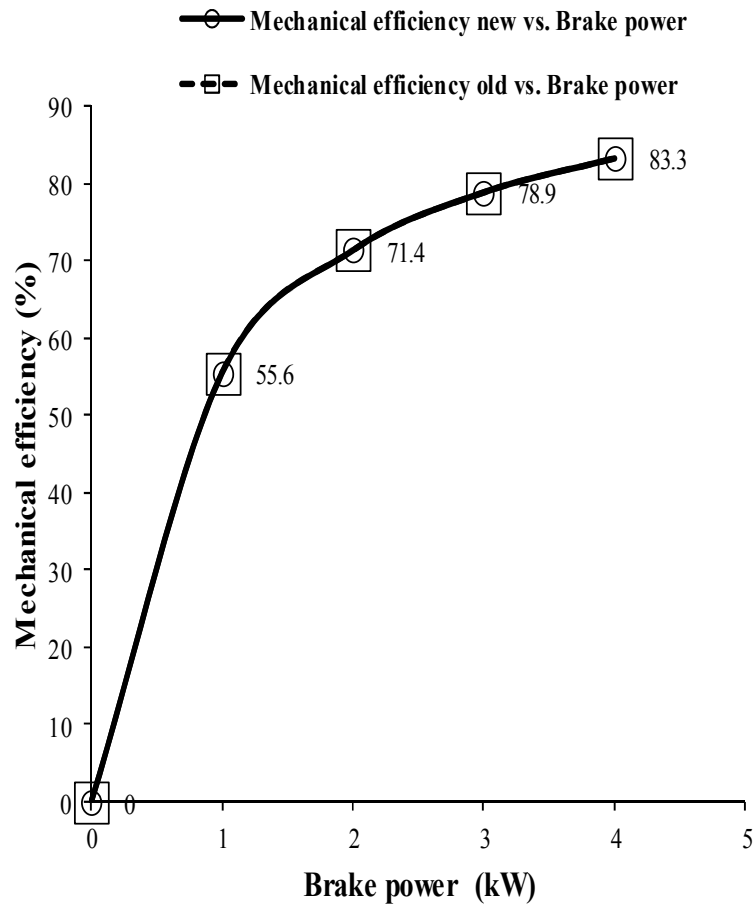


Fig. 19. Variation of Mechanical Efficiency vs. Brake Power.

## 6. Conclusion

It is predicted that split-injection using double lobed cam shows considerable reduction of NO<sub>x</sub> emission from a diesel engine but shows a reverse trend on CO and CO<sub>2</sub> emissions. The results from the experiments have confirmed that the split injection with a 50% split ratio having a 10° crank angle dwell using a double lobbed cam is effective in reducing the NO<sub>x</sub> by 14.1% and UBHC by 11.8% without any appreciable penalty in power.

### Acknowledgement

The authors are thankful to Dr. G. Devaradjane, Professor, Department of Automobile Engineering, Madras Institute of Technology, Chennai, India, for his important input ideas and kind help under whose supervision this work was carried out.

### References

1. Pierpont, D.A.; and Reitz, R.D. (1995). Effects of injection pressure and nozzle geometry on emissions and performance in a diesel. *SAE Paper No. 950604*.
2. Nehmer, D.A.; and Reitz, R.D. (1994). Measurement of the effect of injection rate and split injections on diesel engine soot and NOx emission. *SAE Paper No. 940668*.
3. Tow, T.; Pierpont, A.; and Reitz, R.D. (1994). Reducing particulates and NOx emissions by using multiple injections in a heavy duty D.I. diesel engine. *SAE Paper No. 940897*.
4. Pierpont, D.A.; Montgomery, D.T.; and Reitz, R.D. (1995). Reducing particulate and NOx using multiple injections and EGR in a D.I. diesel. *SAE Paper No. 950217*.
5. Han, Z.; Uludogan, A.; Hampson, G.J.; and Reitz, R.D. (1996). Mechanism of soot and NOx emission reduction using multiple-injection in a diesel engine. *SAE Paper No. 960633*.
6. Gao, Z.; and Schreiber, W. (2001). The effect of EGR and split fuel injection on diesel engine emission. *International Journal of Automotive Technology*, 2, 123-133.
7. Miles, P.; and Dec, J. (1999). Development of innovative combustion process for direct injection diesel engine. *Technical Report No. SAND99-8219*, Sandia National Laboratories, United States.
8. Showry, K.B.; and Raju, A.V.S. (2010). Multidimensional modelling and simulation of diesel engine combustion using multi pulse injections. *International Journal of Dynamics of Fluids*, 6, 237-247.
9. Babu, A.K.; and Devaradjane, G. (2001). Control of diesel engine pollutants by split injection method using multizone model. *SAE Paper No. 2001-28-0007*.
10. Prabhu, T.J. (2005). *Design of transmission element*. Chennai, India: Mani Offset.
11. Ugural, A.C. (2004). *Mechanical design and integrated approach*. New York: McGraw Hill Publication.
12. Rothbart, H.A. (1986). *Mechanical design and system handbook*. New York: McGraw Hill Publication.